

Integration of 3D Intraoperative Ultrasound for Enhanced Neuronavigation

Keith D. Paulsen^{ab}, Songbai Ji^a, Alex Hartov^a, Xiaoyao Fan^a, David W. Roberts^{bc}

^a Thayer School of Engineering, Dartmouth College, Hanover NH 03755, USA

^b Norris Cotton Cancer Center, Dartmouth Hitchcock Medical Center, Lebanon, NH 03756, USA

^c Section of Neurosurgery, Dartmouth Hitchcock Medical Center, Lebanon, NH 03756, USA

ABSTRACT

True three-dimensional (3D) volumetric ultrasound (US) acquisitions stand to benefit intraoperative neuronavigation on multiple fronts. While traditional two-dimensional (2D) US and its tracked, hand-swept version have been recognized for many years to advantage significantly image-guided neurosurgery, especially when coregistered with preoperative MR scans, its unregulated and incomplete sampling of the surgical volume of interest have limited certain intraoperative uses of the information that are overcome through direct volume acquisition (i.e., through 2D scan-head transducer arrays). In this paper, we illustrate several of these advantages, including image-based intraoperative registration (and re-registration) and automated, volumetric displacement mapping for intraoperative image updating. These applications of 3D US are enabled by algorithmic advances in US image calibration, and volume rasterization and interpolation for multi-acquisition synthesis that will also be highlighted. We expect to demonstrate that coregistered 3D US is well worth incorporating into the standard neurosurgical navigational environment relative to traditional tracked, hand-swept 2D US.

Keywords: Ultrasound, Registration, Data Integration for the Clinic/OR, Intraoperative Imaging.

1. INTRODUCTION

Intraoperative ultrasound (iUS) has emerged as a practical navigational tool to account for intraoperative brain shift during open cranial neurosurgical procedures [1–5]. This technique offers real-time image acquisition that integrates seamlessly with neurosurgical workflow and is low in cost. Many studies have shown that iUS plays an important role in complete macroscopic removal of gliomas and metastases [e.g., 6–10]. With the aid of a series of iUS acquisitions, the neurosurgeon is able to compensate for motion of tumor during resection, leading to a more complete removal that ultimately improves patient prognosis and quality of life (e.g., [10]).

Traditionally, two-dimensional iUS (2D iUS) is most commonly used intraoperatively. Because of its planar image acquisition, multiple free-hand sweeps are usually necessary to sample the brain volume of interest. To provide three-dimensional (3D) position and orientation of the acquired iUS, the US transducer is typically rigidly attached with a tracker that is constantly monitored during image acquisition. The series of 2D US images are often combined in order to create a 3D representation of the swept surgical volume. The most dominant methods apply computational reconstruction schemes that interpolate intensity values at a set of regularly spaced Cartesian grid points (see [11] [12] for reviews on various reconstruction algorithms) using voxel-, pixel-, or function-based algorithms [12]. To achieve the best reconstruction results, however, all of these techniques require adequate sampling of the tissue volume, and spurious interpolation may otherwise result when image gaps occur [11]. Confinement of the craniotomy and line-of-sight limitations of the tracking system also create practical constraints which influence the iUS acquisition volume that can be obtained and subsequently reconstructed.

Our group has developed a model-based brain shift compensation scheme that utilizes intraoperative images including ultrasound, stereovision, and fluorescence to aid biomechanical model simulation in order to generate updated MR images for subsequent neuronavigation (Fig. 1) [13]. As part of our overall brain shift compensation strategy, we illustrate the use of volumetric true 3D ultrasonography in this paper and present our recent developments with 3D iUS image acquisition in the context of image-guided neurosurgery.

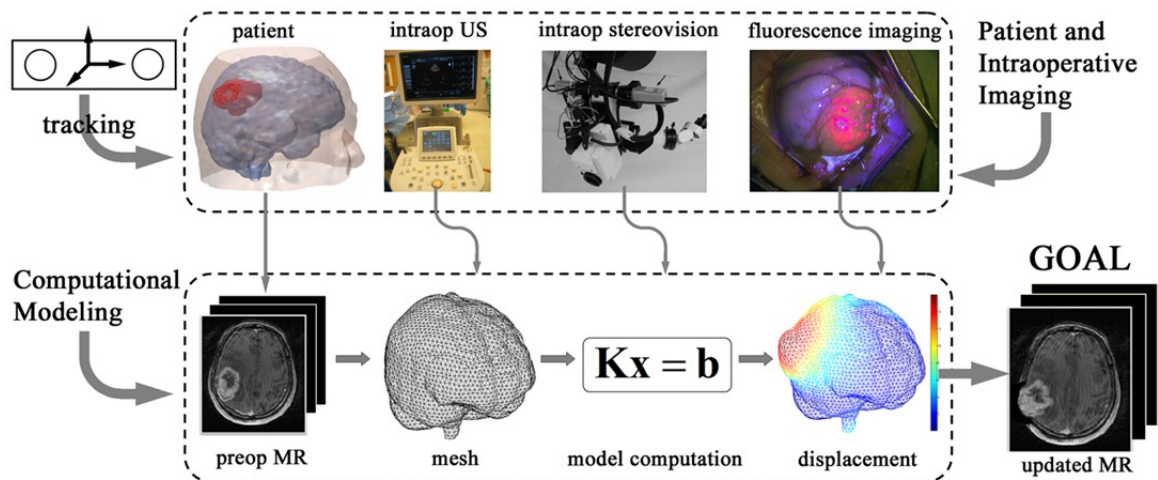


Fig. 1. Overview of a model-based brain shift compensation strategy developed at Dartmouth that incorporates intraoperative ultrasound, stereovision, fluorescence imaging, as well as a subject-specific computational model in order to generate model-updated MR for subsequent neuronavigation [13].

2. METHODS

Volumetric 3D US images are obtained from a Philips iU22 ultrasound system (Fig. 2a; Philips Medical Systems, N.A.; Bothell, WA) through a dedicated 3D US transducer (X3-1; Fig. 2b) that fully samples the imaging volume without the need for free-hand sweeps or 3D reconstruction. In the next sections, we illustrate techniques to rasterize the volumetric data, perform image combination, registration with preoperative MR (pMR) images of the patient’s head, and intra-modality registration with 3D US volumes, from which displacement maps can be extracted and ultimately assimilated into the computational model.

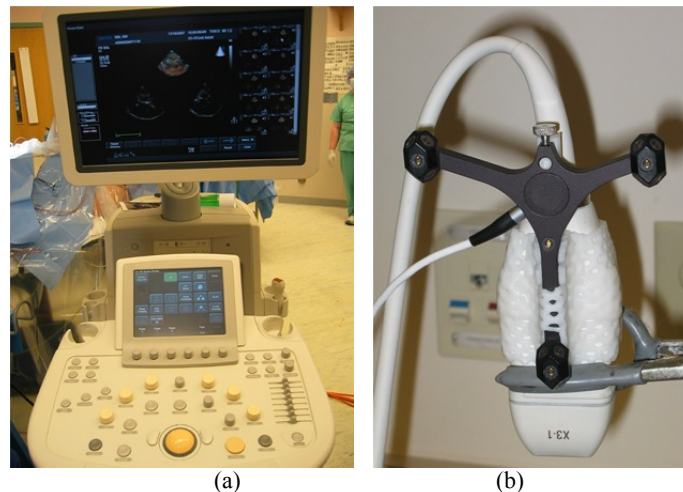


Fig. 2. The iU22 US image acquisition system (a), and an X3-1 broadband matrix array transducer (b). The transducer is rigidly attached with an infrared light-emitting active tracker using Aquaplast thermoplastics, which allows the 3D coordinate position and orientation of the transducer during image acquisition with an optical tracking system.

2.1 Image Rasterization

Understanding the coordinate system of the native 3DUS data is important for processing of the volumetric information. Voxels in volumetric 3D US images are arranged in a non-traditional spherical coordinate system in which a radial distance relative to the origin, O (r ; in mm), a lateral angle (θ ; in degrees), and a medial angle (φ ; in degrees) define a voxel location, which is specified by a triplex $(i_r, j_\theta, k_\varphi)$ where each element denotes an index within the rows, columns

and slices of the 3D image matrix, respectively (point B in Fig. 3). The dimensions of the 3D matrix (i.e., the number of rows, columns and slices) and the physical ranges of the scan-depth (in mm), lateral and medial angles (in degrees) determine the step sizes of r , θ , and φ , respectively. Together with the step sizes, the indices of the voxel in the image matrix determine the position of the voxel (r , θ , φ) in physical space, where r is the distance from the origin, while θ and φ are the angles between the vertical axis OD (the corresponding θ and φ values are both zeros) and planes OBC and OAB , respectively (Fig. 3). Voxels of an iso- θ or iso- φ value are on a plane, whereas voxels of an iso- r value are equidistant from the origin. In the figure shown we have the following geometrical relationships [13]: $OB = r$, $AD = z$, $CD = x$, $OD = y$, $CD \perp OD$ and $AD \perp OD$. In addition, the quadrilateral $ABCD$ is a rectangle, which leads to

$$\begin{cases} x = y \times \tan(\theta), \\ z = y \times \tan(\varphi), \\ x^2 + y^2 + z^2 = r^2. \end{cases} \quad (1)$$

With further manipulation, we have the Cartesian coordinates (x , y , z) from the triplex in the image space (r , θ , φ) determined by

$$\begin{cases} x = y \times \tan(\theta), \\ y = r / \sqrt{1 + \tan(\theta)^2 + \tan(\varphi)^2}, \\ z = y \times \tan(\varphi). \end{cases} \quad (2)$$

Conversely, given the Cartesian coordinates (x , y , z), the image coordinates (r , θ , φ) are

$$\begin{cases} r = \sqrt{x^2 + y^2 + z^2}, \\ \theta = \text{atan}(x/y), \\ \varphi = \text{atan}(z/y). \end{cases} \quad (3)$$

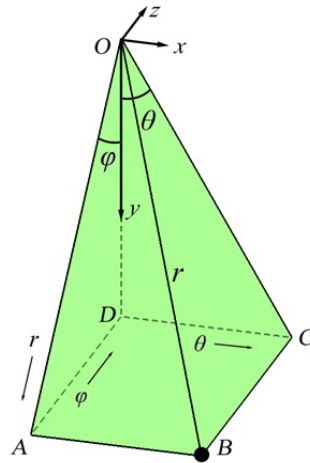


Fig. 3. Illustration of the coordinate system in which a typical 3DUS image voxel (B) is specified by its coordinates (r , θ , φ) [14].

Because volumetric 3D US image voxels are not acquired on a regular grid, rasterization is necessary to resample the image data to allow processing with existing software algorithms. Essentially, rasterization interpolates the image intensities of the volumetric US data onto a uniform grid. This process is performed through a grid space defined as a rectilinear coordinate system where each axis spans from unity to the respective dimension of the image matrix (i.e., the number of rows, columns and slices). The coordinates (i , j , k ; not necessarily integers) of an arbitrary location in grid space that does not necessarily coincide with a grid point, together with the step sizes of r , θ , and φ , uniquely determine

the coordinates in physical space, similarly to voxels located at grid points (Eqns. 4). Conversely, for an arbitrary point in physical space (p in Fig. 4a), the corresponding point in grid space (p' in Fig. 4b) can be uniquely determined (Eqns. 3). This one-to-one mapping establishes the geometrical transformation between the two spaces, allowing the eight neighboring voxels relative to p to be easily identified. In addition, these neighboring voxels form an 8-node hexahedral element in grid space, and the intensity value at p or its equivalent, p' , can then be linearly interpolated using standard finite element trilinear shape functions [13].

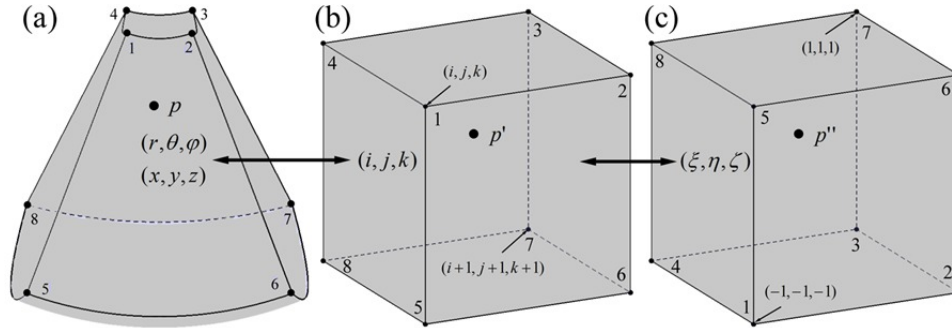


Fig. 4. Sequential transformations of a typical point from physical space (p ; shown in a frustum-shaped volume formed by the eight surrounding voxels) to grid space (p'), and subsequently to natural coordinates (p'') of a hexahedral element determined by the eight surrounding voxels. Image intensity at p is interpolated through the standard trilinear shape functions for a normalized hexahedral element at p in natural coordinates [14].

We have implemented the trilinear interpolation algorithm (TRI), and compared its performance in terms of interpolation accuracy and computational efficiency with two other commonly used approaches – voxel nearest neighbor (VNN) and distance weighting (DW) algorithms. TRI improves interpolation accuracy over both VNN and DW, yet, achieves a real-time computational performance that is comparable to VNN (1–2 orders of magnitude faster than DW) as well as the fastest pixel-based algorithms for processing tracked 2D ultrasound images (0.035 sec per 2D cross-sectional image and 1.05 sec per full volume with 1 mm^3 voxel size; [13]).

2.2 Image Combination

Typically, multiple volumetric 3D US images are acquired at a given surgical stage to increase the sampling region. In this case, combining these images into one volume is preferred for improved computational efficiency of any image processing. In order to combine multiple 3D US acquisitions, a common coordinate system is required, which is accomplished through optical tracking (Northern Digital Inc., London ON, Canada) that continuously monitors two infra-red light emitting sources rigidly coupled with the patient's head (patient tracker) and the US scan-head (US tracker), respectively. Image transformation is illustrated in Fig. 5a, in which ${}^{tracker}T_{US}$ is obtained by transducer calibration (accuracy $\sim 1\text{mm}$; [14]). An arbitrary 3DUS image is transformed into a pre-selected 3D US volume (chosen as the first 3D US image acquired for a patient) coordinate system by

$${}^{US1}T_{US2} = \text{inv}\left({}^{tracker}T_{US}\right) \times \text{inv}\left({}^{patient}T_{tracker}^{(1)}\right) \times {}^{patient}T_{tracker}^{(2)} \times {}^{tracker}T_{US} \quad (4)$$

Apparently, each Cartesian voxel may be physically enclosed by any number of the 3D US acquisitions ($n = 0$, or ≥ 1 ; Fig. 5b). When $n=0$ (i.e., the voxel was not in any 3D US image), a zero-intensity is assigned. Otherwise (i.e., $n \geq 1$), an averaging scheme is used to prescribe a unique intensity value by interpolating across all of the 3D US acquisitions in which the voxel was enclosed.

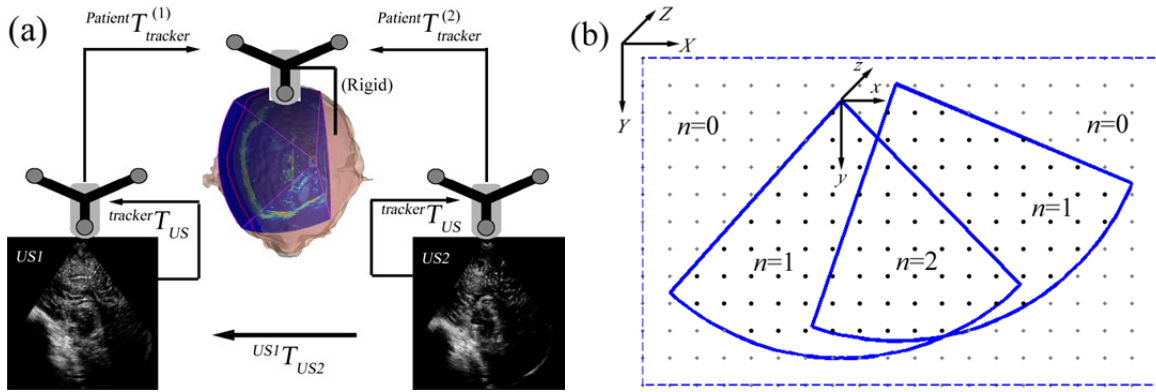


Fig. 5. (a) Illustration of image coordinates involved in transforming 3DUS images. (b) Illustration of image combination and rasterization. Image intensity values of voxels enclosed by multiple 3DUS images ($n \geq 1$) are found by averaging [16].

Because of tracking and calibration errors, two volumetric 3DUS acquisitions may not be perfectly aligned. In order to correct errors in the transformation (i.e., Eqn. 4), inter-image re-registration by maximizing mutual information using the Insight Segmentation and Registration Toolkit is used to place all 3D US volumes into a common coordinate system. The first 3D US acquisition is chosen as the fixed image while all of the rest of the volumes are treated as moving images. In total, $(N-1)$ re-registrations are performed, where N is the number of 3D US acquisitions for a particular patient. Fig. 6 compares the combined and rasterized 3D US images for a typical patient case with and without inter-image registration before image combination and rasterization [15].

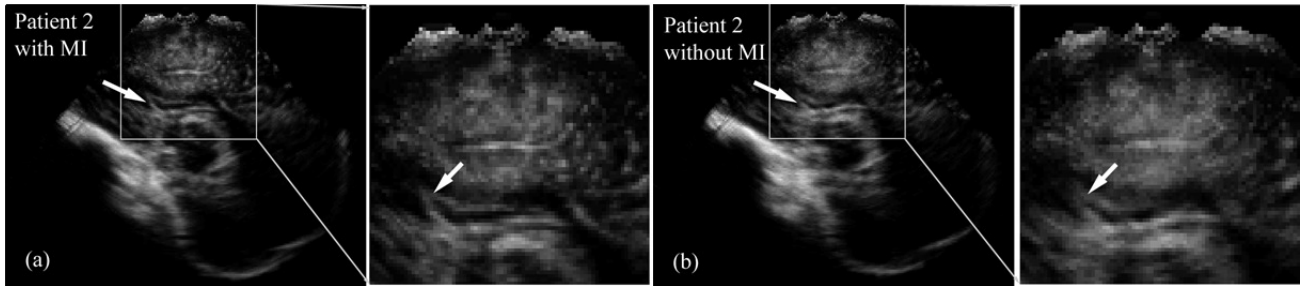


Fig. 6. Combined and rasterized 3DUS images (a) with and (b) without inter-image re-registration for a representative patient. The combined image is significantly sharper when re-registration is applied before rasterization (see arrows and enlarged view of image inset) [16].

2.3 Inter-modality Registration between 3DUS and pMR

Interpretation of intracranial ultrasound can be substantially improved when co-registered with pMR. Because the 3D US transducer is rigidly attached with a tracker, its relative position and orientation with respect to the patient can be determined following concatenation of spatial transformations, once patient registration (e.g., derived from a fiducial-based approach) is available:

$$MR T_{US}^0 = MR T_{patient}^0 \times patient T_{world} \times inv(US_tracker T_{world}) \times US_tracker T_{US}. \quad (5)$$

However, the resulting transformation accumulates errors from the fiducial-based registration itself, US transducer calibration and possible brain motion even at the very start of surgery. To improve the registration accuracy between iUS and pMR, an image based re-registration scheme can be employed to maximize the normalized-mutual-information (nMI) as the image similarity measure. Essentially, the nMI-based re-registration scheme refines the spatial transformation according to

$$\begin{aligned} MR T_{US}^{adjusted} &= T^{adjusted} \times MR T_{US}^0 \\ &= T^{adjusted} \times MR T_{patient}^0 \times patient T_{world} \times inv(US_tracker T_{world}) \times US_tracker T_{US} \end{aligned} \quad (6)$$

as shown in Figure 7.

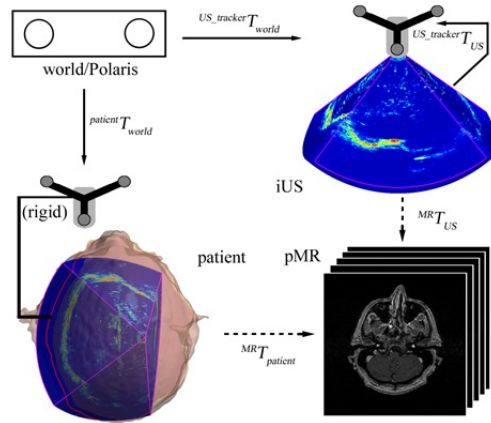


Fig. 7. Coordinate systems involved in image transformations. Solid arrows indicate transformations determined from calibration, and are fixed. Dashed arrows indicate transformations determined from registration, and are subject to adjustment through the nMI-based re-registration scheme. A transformation reversing the arrow direction is obtained by matrix inversion [17].

Figure 8 illustrates the effectiveness of re-registration between 3D US and pMR in order to improve feature alignment between the two image modalities [5].

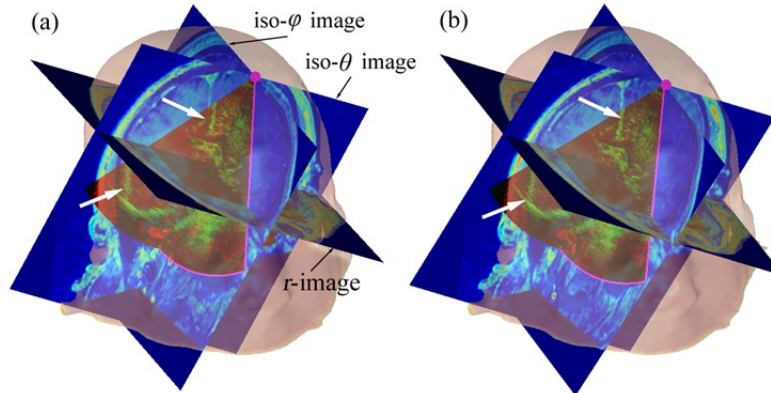


Fig. 8. Composite display using either the fiducial (a) or nMI (b) re-registration. A 3D iUS is overlaid on the corresponding pMR in three planes with respect to the patient scalp surface generated from pMR. The nMI re-registration in (b) significantly improved the alignment of the falx cerebri and parenchymal surface contralateral to the US probe, compared with those in (a) as indicated by the arrows [5].

2.4 Intra-modality image registration between 3D US image volumes

Intra-modality registration between 3D US volumes is important when combining multiple acquisitions into a single volume (see section 2.2). This task is performed by maximizing their mutual information using the ITK toolkit. Image pre-processing includes Gaussian smoothing (kernel of 5×5) of both the fixed and moving images as well as thresholding of the moving images to improve the robustness of the registration. The initial transformation obtained from the tracking system (Eqn. 3) serves as the starting point for re-registration with Mattes version of MI as the image similarity measure. Multithreading is enabled and a steepest gradient descent optimization is employed to maximize MI. Convergence is reached when either the net change in MI is less than 10^{-3} or the number of iterations exceeds a preset maximum value of 200. With image re-registration, the adjusted version of Eqn. 3, which transforms an arbitrary 3D US volume into the coordinate system of the first 3D US acquisition can be written as

$${}^{US1}T_{US2}^{adjust} = T_{adjust} \times \text{inv}\left({}^{tracker}T_{US}\right) \times \text{inv}\left({}^{patient}T_{tracker}^{(1)}\right) \times {}^{patient}T_{tracker}^{(2)} \times {}^{tracker}T_{US} \quad (9)$$

Fig. 9 illustrates the effectiveness of the image re-registration between two volumetric 3D US acquisitions.

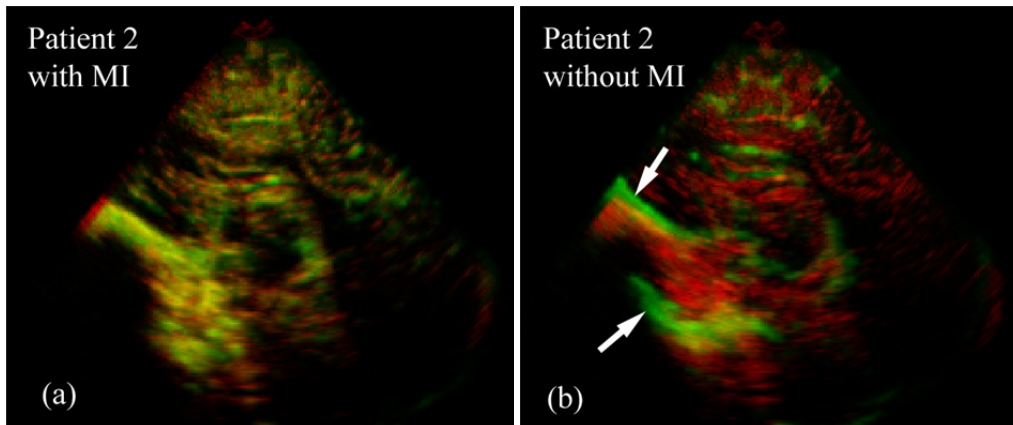


Fig. 9. Significance of registration is apparent when comparing representative overlays of two 3D volumes in the same space generated (a) with or (b) without registration. Arrows in (b) indicate areas of significant misalignment (approx. 3.5 mm) corrected by MI re-registration [16].

Capture ranges are useful measures to assess the robustness of the registration and can be determined by the perturbation method [16] where the floating 3D US image is perturbed away from its converged location from a successful registration relative to the fixed image and the image registration is executed again. After the registration converges, the new location of the floating image relative to the fixed image, or the average distance error, is plotted against the magnitude of the initial translational and rotational misalignment (e.g., see Fig. 10). This allows the corresponding capture ranges, defined as the maximum initial misalignment where at least 95% of the perturbed registrations are successful (successful registration is defined as the average distance error ≤ 2 mm), to be determined. For 3D US images, we found that these intra-modality registration capture ranges are 35.2 mm and 32.8 deg, respectively, which are similar to those in reports of reconstructed 3DUS images in the literature (25.5 mm [17] and 40 deg [18]) and much larger than those we have obtained when re-registering tracked 2D US.

2.5 Displacement Mapping from 3D US Image Volumes

An important application of volumetric 3D US is extraction of feature displacement maps to guide the model computations in Figure 1. A "last-known" correct registration between 3D US and pMR is important before dural opening in order to collectively correct any misalignment due to errors in patient registration and US transducer calibration. This registration defines the spatial transformation required to transform displacement maps from the 3D US image space into the pMR image space (see section 2.3 for details).

In order to compute feature displacements, a typical 3D US image volume acquired at a particular surgical stage is spatially transformed into the image space of the 3D US image volume obtained before dural opening (i.e., chosen as the fixed image volume in registration) using the transformation provided by the tracking system. Because of errors in 3D US image acquisition and tracking, stationary or immobile features may be misaligned, which potentially degrade accuracy in the feature displacement measurements. To compensate for this misalignment, a simple rigid body registration is performed between the two image volumes by limiting the region of interest to the stationary features (e.g., parenchymal boundaries contralateral to the craniotomy/US transducer; see Fig. 11a). In practice, portions of the image volume contralateral to the US transducer (i.e., corresponding to stationary features) are employed for image re-registration purposes. The two 3D US image volumes are then re-aligned, and any residual feature misalignment directly indicates tissue deformation (see Fig. 11b). Depending on the severity of nonrigid deformation, either a rigid (e.g., after dural opening; fast and robust but less accurate) or a nonrigid (e.g., after partial or complete tumor resection; slow but likely more accurate) registration can be performed between the two 3D US image volumes after rigid re-registration (based on the stationary features). A B-spline nonrigid registration may be preferred because it provides a smooth deformation field that is desirable when assimilating the displacement data to estimate whole-brain deformation. Fig. 11c illustrates feature alignment after nonrigidly registering two 3D US image volumes, and Fig. 11d shows the resulting displacement vectors in areas under the craniotomy where parenchymal distension was evident.

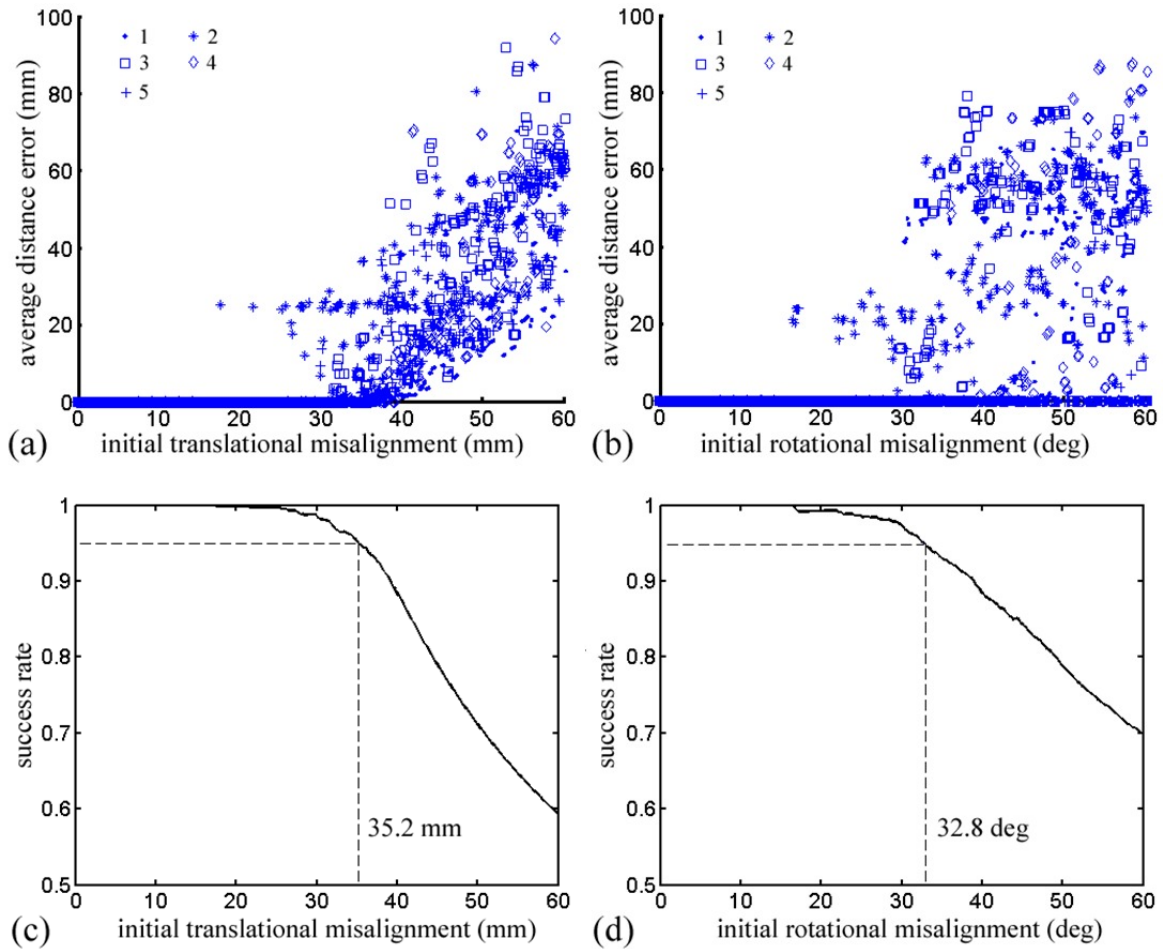


Fig. 10. Scatter plots of average distance error vs. initial (a) translational and (b) rotational misalignment, along with the corresponding (c) translational and (d) rotational success rate curves [16].

Because of the higher cost of computations with nonrigid registration, only the region of interest (e.g., around tumor or ventricles) is used for registration (where automatic and efficient segmentation of iUS is achievable), or a partial region under the craniotomy (e.g., scan depth between 1–6 cm instead of the full volume). Based on the displacement mapping, a randomly generated subset of voxels that are representative of the regional deformation can then be produced for data assimilation to further reduce the computational overhead [19].

2.6 Incorporating Volumetric 3D US into Model-based Brain Shift Compensation

Feature displacement maps extracted from 3D US are ultimately assimilated into a biomechanical model in order to guide model deformation. Here, we illustrate a patient case utilizing sparse data generated from both 3D US (for features deep in the brain) and intraoperative stereovision, iSV, (for exposed parenchymal surface) towards the end of tumor resection. Whole-brain deformation was computed using an inverse biomechanical model with sparse data generated from both 3D US and iSV, from which model-updated MR images (uMR) were generated. To assess the accuracy of the model computation, the uMR was overlaid with 3D US on a sagittal plane as well as with the cross-section of the parenchymal cavity surface obtained from iSV (Fig. 13). The consistency between features found in these three image modalities suggests sufficient accuracy of the model computation and the effectiveness of utilizing intraoperative images for model guidance.

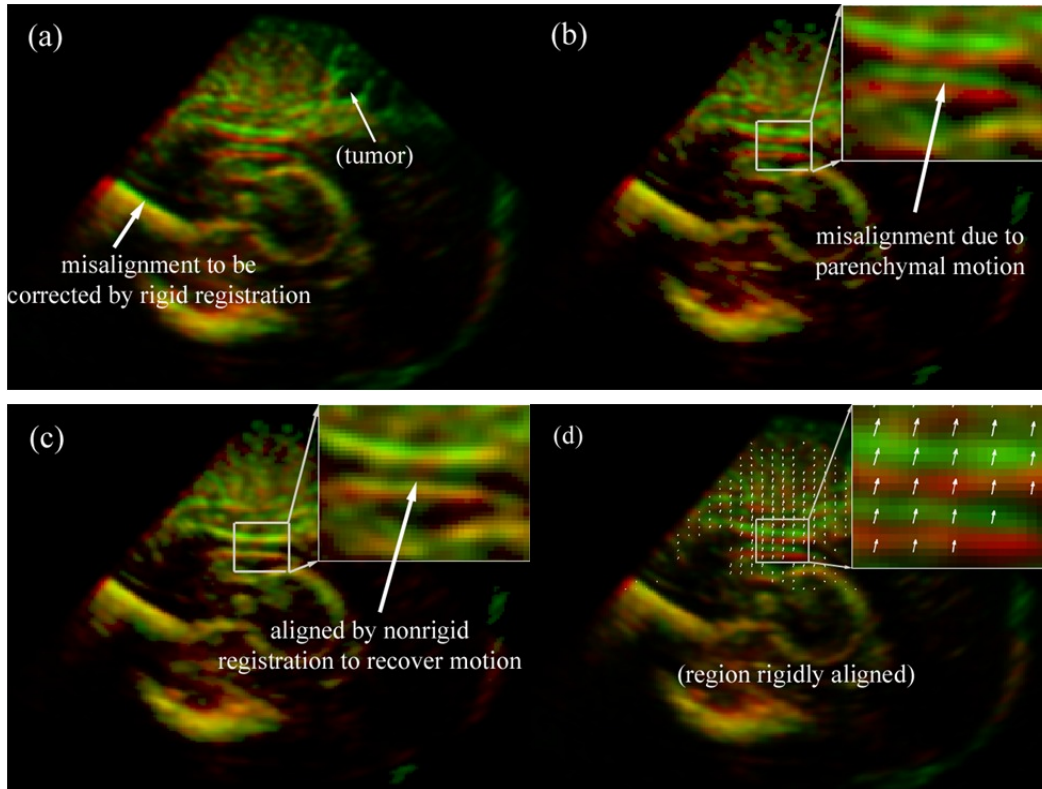


Fig. 11. Overlays of 3D US before (red) and after (green) dural opening using transforms obtained from the optical tracking (a) or rigid body re-registration (b). Feature alignment is significantly improved after B-Spline nonrigid registration (c), suggesting the effectiveness of the registration technique in capturing feature displacement. The resulting parenchymal feature displacement vectors are shown in (d) [20].

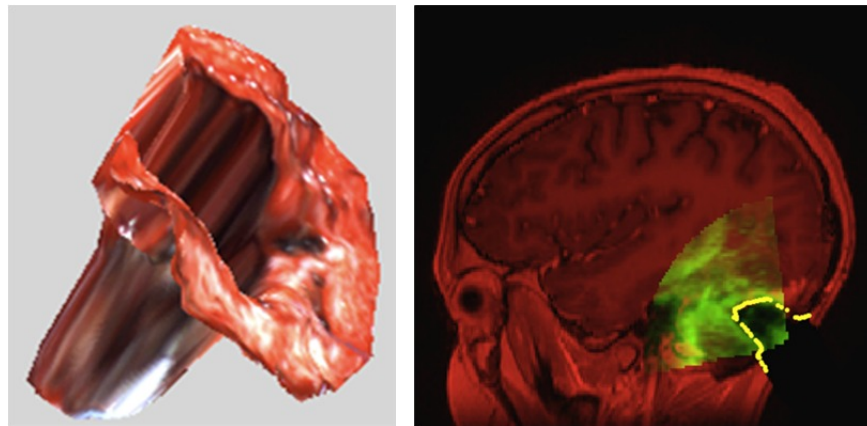


Fig. 12. Left: surface profile of the tumor cavity obtained from stereovision; Right: overlay of model-updated MR (red) and 3D US (green) on a sagittal plane; also shown is the cross-section of the surgical cavity surface from stereovision in the same sagittal view [20].

3. DISCUSSION AND CONCLUSION

Ultrasonography has emerged as an important and practical intraoperative imaging technique for use in neurosurgery. Because volumetric true 3D ultrasound samples the surgical region of interest uniformly within the brain without the need for freehand sweeps, it is more reliable and robust for subsequent image processing and analyses that can enhance neurosurgical guidance. In this paper, we have described the integration and use of volumetric true 3D US in our image-guidance data acquisition to aid neuronavigation in the OR. Unlike conventional 2D US where multiple free-hand sweeps are usually required to sample the region of interest and computational reconstruction is often used to generate a 3D representation of the imaged volume, 3D US acquisition provides “true” volumetric sampling of the target tissue. The approach is also significantly more efficient, which is of practical importance for routine use in the OR.

We have illustrated the use of volumetric 3DUS and presented some recent developments that capitalize on this imaging technique in the context of image-guided neurosurgery. Specifically, co-registering volumetric 3D US with pMR improves the interpretation and understanding of intracranial features, similarly to traditional 2D ultrasound images. Registration performance between 3D US volumes is robust with translational and rotational capture ranges that reach 35.2 mm and 32.8 deg. Intra-modality registration between 3D US is helpful when combining multiple acquisitions into a single volume because it effectively reduces image blurring of distinct intracranial features. In addition, direct (and robust) image registration of 3D US volumes acquired at two different surgical stages can be used to automatically extract displacement maps as motion information for data assimilation.

Overall, we find that coregistered 3D US is well worth incorporating into the standard neurosurgical navigational environment relative to traditional tracked, hand-swept 2D US, and that technological advances in volumetric 3D US image processing techniques are important to ultimately incorporate data extracted from the technique into a model-based brain shift compensation strategy for improved neurosurgical navigation.

4. ACKNOWLEDGEMENT

Funding from National Institutes of Health grant R01 CA159324-01 is acknowledged.

REFERENCES

1. Bonsanto, M.M., Staubert, A., Wirtz, C.R., Tronnier, V., and Kunze, S.: Initial experience with an ultrasound-integrated single-rack neuronavigation system. *Acta Neurochirurgica*, **143**(11) (2001) 1127–1132
2. Bucholz, R.D., Smith, K.R., Laycock, K.A., and McDermont, L.L.: Three-dimensional localization: From image-guided surgery to information-guided therapy. *Methods (Duluth)*, **25**(2) (2001) 186–200
3. Comeau, R.M., Sadikot, A.F., Fenster, A., and Peters, T.M.: Intraoperative ultrasound for guidance and tissue shift correction in image-guided neurosurgery. *Medical Physics*, **27** (2000) 787–800
4. Rasmussen, I.A. Jr., Lindseth, F., Rygh, O.M., Berntsen, E.M., Selbekk, T., Xu, J., Nagelhus Hernes, T.A., Harg, E., Håberg, A., Unsgaard, G.: Functional neuronavigation combined with intra-operative 3D ultrasound: initial experiences during surgical resections close to eloquent brain areas and future directions in automatic brain shift compensation of preoperative data. *Acta Neurochir (Wien)*. **149**(4) (2007) 365-78
5. Ji, S., Fontaine, K., Hartov, A., Borsic, A., Roberts, D.W., and Paulsen, K.D.: Coregistered volumetric true 3D ultrasonography in image-guided neurosurgery. *Medical Imaging 2008: Visualization, Image-Guided Procedures, and Modeling*, edited by Michael I. Miga, Kevin R. Cleary, Proceedings of SPIE Vol. 6918 (SPIE, Bellingham, WA 2008) 69180F.
6. Lacroix, M., Abi-Said, D., Fourney, D.R., Gokaslan, Z.L., Shi, W., DeMonte, F., Lang, F.F., McCutcheon, I.E., Hassenbush, S.J., Holland, E., Hess, K., Michael, C., Miller, D., and Sawaya, R., A multivariate analysis of 416 patients with glioblastoma multiforme: prognosis, extent of resection and survival, *J Neurosurg*, 2001, 95, 190-198.
7. Buckner J.C., Factors influencing survival in high grade gliomas, *Semin. Oncol.* 30:10-14,2003.
8. Laws E.R., Shaffrey M.E., Morns A., Anderson F.A. Jr., Surgical management of intracranial gliomas – does radical resection improve outcome?, *Acta Neurochir Suppl*, 85:47-53, 2003.
9. C. Renner, D. Lindner, J.P. Schneider and J. Meixensberger, “Evaluation of intra-operative ultrasound imaging in brain tumor resection: a prospective study,” *Neurological Res.*, 27:351-357, 2005.
10. Unsgaard A., Rygh, O.M., Selbekk T., Buller T.B., Kolstad F., Lindseth, F., and Nagelhus Hernes T.A., Intraoperative 3D ultrasound in neurosurgery, *Acta Neurochirurgica*, 148:235-253, 2006.
11. Fenster A., Downey D.B., and Cardinal H.N., Three-dimensional ultrasound imaging, *Phy. Med. Bio.*, 46:R67-R99, 2001.

12. Solberg O.V., Lindseth F., Torp H., Blake R.E., and Nagelhus Hernes T.A., Freehand 3D ultrasound reconstruction algorithms – a review., *Ultrasound Med. Biol.*, 33(7):991-1009, 2007.
13. Ji S., Fan X., Fontaine K., Hartov A., Roberts D.W., Paulsen K.D., "An integrated model-based neurosurgical guidance system" in Medical Imaging 2010: Visualization, Image-Guided Procedures, and Modeling, edited by Kenneth H. Wong, Michael I. Miga, Proceedings of SPIE Vol. 7625 (SPIE, Bellingham, WA 2010) 762536.
14. Ji, S., Roberts, D.W., Hartov, A., Paulsen, K.D.: Real-time Interpolation for True 3-Dimensional Ultrasound Image Volumes. *Journal of Ultrasound in Medicine* **30** (2011) 241–250
15. Hartov, A., Paulsen, K.D., Ji, S., Fontaine, K., Furon, M., Borsic, A., Roberts, D.W.: Adaptive Spatial Calibration of a 3D Ultrasound System. *Med. Phys.* **37**(5) (2010) 2121–2130
16. Ji, S., Roberts, D.W., Hartov, A., Paulsen, K.D.: Combining multiple volumetric true 3D ultrasound volumes through re-registration and rasterization. G.-Z. Yang et al. (Eds.): MICCAI Part I, LNCS **5761** (2009) 795–802
17. Ji, S., Wu, Z., Hartov, A., Roberts, D.W., Paulsen, K.D.: Mutual-information-based patient registration using intraoperative ultrasound in image-guided neurosurgery. *Medical Physics*. **35**(10) (2008) 4612–4624
18. Shekhar R, and Zagrodsky V, Mutual information-based rigid and nonrigid registration of ultrasound volumes. *IEEE Tran. Med. Imag.* 21(1):9–22, 2002.
19. Slomka PJ, Mandel J, Downey D, and Fenster A, "Evaluation of voxel-based registration of 3-D power Doppler ultrasound and 3-D magnetic resonance angiographic images of carotid arteries," *Ultrasound in Med. & Biol.*, 27(7):945–955, 2001.
20. S. Ji, X. Fan, A. Hartov, D.W. Roberts, and K.D. Paulsen. "Estimation of intraoperative brain deformation", "Soft Tissue Biomechanical Modeling for Computer Assisted Surgery", to be published by Springer in the framework of the Series "Studies in Mechanobiology, Tissue Engineering and Biomaterials". (Accepted).